Journal Pre-proofs

Levofloxacin in nanostructured lipid carriers: preformulation and critical process parameters for a highly incorporated formulation

Viviane Lucia Beraldo de Araújo, Ana Flávia Siqueira Vicente, Marcelo van Vliet Lima, Anita Umerska, Eliana Barbosa Souto, Lidia Tajber, Laura de Oliveira Nascimento

PII: S0378-5173(22)00747-5
DOI: https://doi.org/10.1016/j.ijpharm.2022.122193
Reference: IJP 122193

To appear in: *International Journal of Pharmaceutics*

Received Date: 16 February 2022
Revised Date: 5 August 2022
Accepted Date: 7 September 2022

Please cite this article as: V. Lucia Beraldo de Araújo, A. Flávia Siqueira Vicente, M. van Vliet Lima, A. Umerska, E. Barbosa Souto, L. Tajber, L. de Oliveira Nascimento, Levofloxacin in nanostructured lipid carriers: preformulation and critical process parameters for a highly incorporated formulation, *International Journal of Pharmaceutics* (2022), doi: https://doi.org/10.1016/j.ijpharm.2022.122193

Levofloxacin in nanostructured lipid carriers: preformulation and critical process parameters for a highly incorporated formulation

Viviane Lucia Beraldo de Araújo[a,b,c], Ana Flávia Siqueira Vicente[a], Marcelo van Vliet Lima[a,d], Anita Umerska[b], Eliana Barbosa Souto[e,f], Lidia Tajber[b*], Laura de Oliveira Nascimento[a]

[a]Faculty of Pharmaceutical Sciences, State University of Campinas, Campinas, Brazil

[b]School of Pharmacy and Pharmaceutical Sciences, Trinity College Dublin, College Green, Dublin 2, Ireland

[c]Centre of Biological Engineering (CEB), University of Minho, Campus de Gualtar, 4700 Braga, Portugal

[d]Sanofi Medley Farmacêutica Ltda, Campinas, Brazil

[e]Department of Pharmaceutical Technology, Faculty of Pharmacy, University of Porto, Rua de Jorge Viterbo Ferreira, 228, 4050-313 Porto, Portugal

[f]REQUIMTE/UCIBIO, Applied Molecular Biosciences Unit, Faculty of Pharmacy, University of Porto, Rua de Jorge Viterbo Ferreira, 228, 4050-313 Porto, Portugal

* Corresponding author, Lidia Tajber, School of Pharmacy and Pharmaceutical Sciences, Trinity College Dublin, College Green, Dublin 2, Ireland. Tel: +35318962787. Email: ltajber@tcd.ie

Abstract

The first step of a successful nanoformulation development is preformulation studies, in which the best excipients, drug-excipient compatibility and interactions can be identified. During the formulation, the critical process parameters and their impact must be studied to establish the stable system with a high drug entrapment efficiency (EE). This work followed these steps to develop nanostructured lipid carriers (NLCs) to deliver the antibiotic levofloxacin (LV). The preformulation studies covered drug solubility in excipients and thorough characterization using thermal analysis, X-ray diffraction and spectroscopy. A design of experiment based on the process parameters identified nanoparticles with < 200 nm in size, polydispersity <= 0.3, zeta potential -21 to -24 mV, high EE formulations (> 71%) and an acceptable level of LV degradation products (0.37-1.13%). To the best of our knowledge, this is the first time that a drug degradation is reported and studied in work on nanostructured lipids. LV impurities following the NLC production were detected, mainly levofloxacin N-oxide, a degradation product that has no antimicrobial activity and could interfere with LV quantification in spectrophotometric experiments. Also, the achievement of the highest EE in lipid nanoparticles than those described in the literature to date and the apparent protective action of NLC of entrapped-LV against degradation are important findings.

Keywords: preformulation, design of experiments, levofloxacin, nanostructured lipid carrier, solid state, degradation

1. Introduction

Over the last decades, nanostructuring of pharmaceuticals maintains a prominent status as an effective drug delivery strategy. As a result, a range of different types of nanostructures have been developed and studied for this purpose. Examples include liposomes, nanoemulsions, nanotubes, nanomicelles, lipid and polymeric nanoparticles, nanotubes, etc. (Li et al., 2017). Comparing the various types of pharmaceutical nanostructures, lipid nanoparticles (NPs) play a key role due to their particular advantages. They comprise ingredients that are usually biocompatible, biodegradable and have low potential toxicity; the technology might be translated into a large-scale production; can modify and control drug release; enhance drug solubility and are able to incorporate both hydrophilic and lipophilic molecules. Furthermore, the dispersion stabilization is afforded by a mixture of surfactants and cosurfactants (Müller et al., 2000).

Levofloxacin (LV) is a fluoroquinolone drug first introduced in 1993. It shows a broad spectrum of action and is commonly used to treat respiratory, urinary tract, skin and soft tissue bacterial infections. The most common LV side-effects are nausea, diarrhea, headache, but also rare severe effects, such as tendinitis and tendon rupture (Liu, 2010). These pitfalls of LV have encouraged, especially in the past ten years, several studies aiming at incorporating LV into nanoparticles of several types, including polymeric and lipidic systems. Abdel Hady et al. were able to co-incorporate LV and docycycline into solid lipid nanoparticles (SLNs) and to improve the brain targeting via the nose-to-brain route in comparison to the intravenous administration (Abdel Hady et al., 2020). In the study of Ameeduzzafar et al., LV-loaded chitosan NPs showed better results regarding the corneal clearance, drug retention and naso-lachrymal drainage in ocular delivery compared to the LV solution (Ameeduzzafar et al., 2018). Islan et al. produced SLN and nanostructured lipid carriers (NLC)-loaded LV with DNase type I, which reduced the lung viscoelasticity, exacerbated in cystic fibrosis patients, and the formation of bacterial biofilm (Islan et al., 2016). Kumar et al. studied lyophilized NPs of PLGA to deliver LV by the oral route (Kumar et al., 2012). Moreover, lipid nanoparticles were able to prevent the crystallization of LV free drug at the high administered concentrations, reducing the risks of LV-induced crystal nephropathy (Liu et al., 2015).

Unfortunately, the published accounts on LV nanostructures also suffer from drawbacks. From the total of 30 studies on LV NPs analyzed in past 10 years, only 19 determined the entrapment efficiency (EE) of the drug, 15 presented the drug loading and only one presented the drug content in the final formulation to determine EE (Zhang et al., 2019). These data are important to explain the achieved outcomes, to be reliable and reproducible for other researchers. Another concern, when comes to formulating NPs, is the scarceness of studies

on the drug degradation during the formulation step. Drug degradation and total drug content also allow us to evaluate the compatibility of drug with excipients and the process parameters that affect the stability of such mixtures. There are few studies reporting that the high temperature during NLC process may promote drug degradation of labile molecules such as astaxanthin (Dhiman et al., 2021; Tamjidi et al., 2014), but no similar studies have been done for LV NPs. For LV, the most common degradation product is levofloxacin N-oxide (LNO). This substance has no antibiotic activity and absorbs UV light at the same wavelength as LV, the reason why spectrophotometric methods with no separation of molecules can hinder degradation (Czyrski et al., 2019).

Although the importance of nanosystems in commercial formulations has not been fully realized yet, a few products have been marketed, for instance Doxil, liposomal doxorubicin and Abraxane, paclitaxel nanoparticles, both approved for the clinical use (Li et al., 2017). Also, the state of art in analytics has improved over time. The improvements and rising rigor from the controlling agencies led to the adoption of Quality by Design (QbD) approach (Q3B/8/9/10/11) and the mandatory drug stability indicating assay, among others, to enable a production of a safe and good quality product (Cunha et al., 2020). However, it is regrettable that academic studies do not have to follow these rules and the published accounts vary in degree of analytical data and often prioritize biological outcomes. Thus, the factors that influence the physicochemical characteristics of nanoformulations and their consequences are not completely clear, hindering the possibility of a clinical translation and industrial production, which must follow the guidelines for quality standards and reproducibility (Li et al., 2017). Nevertheless, a considerable number of articles have recently been published describing the QbD approach in the development of lipid nanoparticles, measuring the impact of formulation composition, such as the lipids and surfactant content, on the parameters intrinsic to the biological performance of NPs (nanoparticle size, polydispersity index (PdI), zeta potential and entrapment efficiency (EE)). The process variables are also key to be considered during optimization processes, including the number of cycles, the rate and duration of emulsification and, if sonication is used, the amplitude and time of the sonication process (Cunha et al., 2020). The QbD begins to be valued in the field of pharmaceutical NPs as an important tool to help the understand the products and processes, building the quality into the production and following the standards (Li et al., 2017).

For these reasons, this paper focused on the preformulation studies (excipient selection) and process production parameters of nanostructured lipid carriers loaded with LV, evaluating, for the first time, the presence degradation products induced by the formulation process. Critical material attributes (CMA) were studied by selecting biodegradable and non-toxic excipients, screened by the criteria of drug solubility and solid-state analyses. Afterwards, based on the

drug-lipid solubility, we determined the formulation critical quality attributes (CQA) according to the NP size, polydispersity, zeta potential and entrapment efficiency. The formulation composition and the process of production were further evaluated considering the selected CMAs and critical process parameters (CPPs) (the sonication time, amplitude and temperature), analyzing the CQAs based on literature and previous studies of the group. We also evaluated formulation stability, sorption kinetics, *in vitro* drug release and the production of total impurities depending on the CPPs.

2. Material and methods

2.1 Materials

Levofloxacin hemihydrate (LV, (2S)-7-fluoro-2-methyl-6-(4-methylpiperazin-1-yl)-10-oxo-4-oxa-1-azatricyclo [7.3.1.$0^{5,13}$]trideca-5(13),6,8,11-tetraene-11-carboxylic acid hemihydrate) was purchased from FluoroChem (UK) and also generously donated by Sanofi-Medley Farmacêutica Ltda from Brazil. Levofloxacin N-oxide standard was purchased from Eurobram (Germany). Oleic acid was purchased from Dinâmica Química Contemporânea Ltda (Brazil). Super Refined™ polysorbate-80, Super Refined™ oleic acid, beeswax and Crodamol™ CP (cetyl palmitate) were donated by Croda (UK). Precirol® ATO 5, Compritol® 888 ATO, Geleol™ mono and diglycerides, Gelucire® 50/13 (stearoyl polyoxylglycerides) and Biogapress Vegetal BM 297 ATO (glyceryl dipalmitostearate) were donated by Gattefossé (France), while Tego® care 450 (polyglyceryl-3 methylglucose distearate) was donated by Evonik. Dynasan® 116 (glyceryl tripalmitate) and Dynasan® 118 (glyceryl tristearate) were provided by IOI Oleochemical (Germany). Stearic acid and phosphate buffered saline (PBS) sachets were purchased from Sigma-Aldrich (Germany) (one sachet dissolved in 1000 mL of deionized water yields 0.01 M phosphate buffer, KCl 0.0027 M and NaCl 0.137 M sodium chloride, pH 7.4, at 25 °C). Potassium bromide (KBr) of infrared grade was obtained from Sigma-Aldrich (Ireland). All other chemicals and solvents were of analytical grade.

2.2 Methods

Pre-selection of excipients

The determination of LV solubility in lipids was made by mixing 1 or 5 mg (1 or 5% w/w, respectively) of drug with each of the excipients to make a total of 100 mg mixture in a 10 mL glass test tube. The mixtures were kept in a heated water bath (J.P. Selecta Precisterm series, Spain) at 80 °C for 60 minutes. The pre-selection of excipients was made after visually checking LV solubilization in the mixtures every 15 min. The formation of a clear, pale-yellow mixture was deemed as indication of LV solubility in that excipient. A cloudy mixture or a

system containing visible LV particles indicated a partially soluble or insoluble system, respectively.

Thermal analysis

Differential scanning calorimetry (DSC) of the bulk materials, physical, binary mixtures of 5% LV-excipient systems and NLCs were performed using Mettler Toledo DSC 821^e model with a refrigerated cooling system LabPlant RP-100 (Mettler-Toledo GmbH, Switzerland) with samples of 3-5 mg weighted in 40 mL pierced lid aluminum pans. The analyses were carried out under nitrogen flow. Physical mixtures of 5% LV-excipient were prepared using an agate mortar with a pestle. The heating program started from -35 or 25 °C, depending on the sample, up to 300 °C, and a heating rate of 10 °C/min was used for all systems. The samples were weighted on microanalytical balance Mettler Toledo, XP6 model (Mettler-Toledo, Switzerland). Thermograms were evaluated as onset temperatures for melting events and heat of transitions was also determined.

Thermogravimetry (TGA) of the bulk materials, physical mixtures and the NLC samples was performed to evaluate their thermal stability. The starting decomposition temperature was that up to which a maximum of 5% w/w mass loss was measured (Umerska et al., 2020a). Analyses were carried out in a Mettler Toledo TG50 measuring module coupled to a Mettler Toledo MT5 balance. Samples weighing 8−10 mg were placed in 40 µL open aluminum pans and heated from 25 to 300 °C at a rate of 10 °C/min under nitrogen flow as the purge gas with a flow rate of 40 mL/min. Mettler Toledo STAR^e software (version 6.10) was used to identify the weight loss based on the slope of TGA trace. TGA was also used to pre-heat the physical mixtures at NLC preparation conditions (58 °C, 30 min) before analyzing them by powder X-ray diffraction as well as infrared analysis and compared to the non-heated mixtures.

X-ray diffraction (XRD)

Powder XRD measurements were performed using a Rigaku Miniflex II, desktop X-ray diffractometer (Japan), equipped with an X-ray source using CuKα radiation at 30 kV and 15 mA, with a Haskris cooling unit. Diffractograms were acquired over the 2 θ range between 2° - 40° at a step size of 0.05° per second. This method was adapted from (Umerska et al., 2020b).

Infrared analysis (FTIR)

FTIR analyses allowed to identify the functional groups of the samples (bulk or mixtures excipient-LV 5% w/w). The peaks in the absorption spectra were obtained from KBr discs with approximately 10% w/w of sample loading, prepared by compression using a hydraulic IR press (40 bar for 1-2 min). The spectral range recorded was 4000-650 cm^{-1}, accumulation of

10 scans and resolution of 16 cm^{-1} was applied. Spectra were recorded on a Spectrum One spectrometer (Perkin Elmer, USA). Following collection, background correction and intensity normalization were applied to the data using Spectrum v. 5.0.1 software.

Design of experiments (DoE) approach

A full factorial 2^3 design was performed to optimize the properties of the NLC formulation and determine the CMAs. The inputs (variables) were: the amount of total lipids in the formulations (the lipid to aqueous phase ratio: 0.5, 0.75 and 1.0 g of lipids to 10 g of aqueous phase), proportion of solid and liquid lipids (70:30, 80:20 and 90:10 w/w), and the amount of surfactant (2, 3 and 4% w/v). They were evaluated at 2 levels of concentrations and a triplicate on the center point (intermediate concentration) was also tested. The order of preparation was randomized. The outputs evaluated to determine the best formulation were z-average size, polydispersity index (PdI), zeta potential and entrapment efficiency (EE). The desirable outputs to choose the best formulation were z-average < 250 nm, PdI < 0.3 and the highest EE value. The results were analyzed by software Minitab® 17.1.0.

A second full factorial 2^3 design was run to optimize the process parameters of NLCs, thus determine CPPs. The best formulation parameters determined in the first DoE were employed in this factorial design. The independent variables were: the temperature, sonication time and sonication amplitude. For the temperature parameter, the values chosen were such to represent conditions in which the solid lipid would be solid (38 °C) or melted (58 and 78 °C). The usual sonication time applied by our group is 30 min (Beraldo-de-Araújo et al., 2019), however, 20 minutes was also considered. Finally, the sonication amplitude varied to verify its influence on the physicochemical parameters (outputs). The outcomes examined were z-average size, PdI, zeta potential, EE and total impurities, analyzed by software Minitab® 17.1.0.

NLC production

NLCs were prepared by the hot emulsification-ultrasonication method (Beraldo-de-Araújo et al., 2019; Schwarz et al., 1994). Shortly, the lipid phase components (the solid and the liquid lipids) were melted in a beaker over a water bath at 58 ± 2 °C and LV was added under magnetic stirring. The aqueous phase was prepared in another beaker, containing water and the surfactant, heated on a hot plate under magnetic stirring and this solution was added to the lipid phase under mixing, 12,000 rpm for 3 min, in an Ultraturrax blender (IKA® T18 basic, Germany) using the S18N-19G dispersing tool. This emulsion was then sonicated using a tip sonicator (Vibracell, Sonics & Materials Inc., USA) fitted with a 3 mm probe. The following conditions of processing were used: power 130 W and 20 kHz nominal frequency; cycling of

30 seconds (on/off) for 30 minutes at an amplitude of 50%. The dispersion was then cooled to 25 ºC over an ice bath and stored at room temperature protected from the light.

NLC characterization

Determination of hydrodynamic diameter (z-average), dispersity (PdI) and zeta potential (ZP)

Z-average size was determined by Dynamic Light Scattering (DLS) (Zetasizer Nano ZS90, Malvern Instruments Ltd, UK), at a 90° scattering angle and 25 °C, using a disposable polystyrene cuvette, with samples diluted to 1:200 in sodium chloride 10 mM or milliQ water (refraction index 1.332 – viscosity 0.8910 cP) to reach an adequate correlation coefficient (between 0.7–1). The zeta potential (ZP) of these diluted samples was determined by the same instrument, measuring the electrophoretic mobility using a disposable polystyrene cuvette model DTS1070 with electrodes. The samples were measured in triplicate and results presented as mean ± standard deviation.

Determination of LV concentration by High Performance Liquid Chromatography (HPLC)

LV was measured using HPLC, as described in the United States Pharmacopoeia (USP) monograph for Levofloxacin Tablets ("Levofloxacin," 2017). The analyses were performed using the Prominence-i LC2030C, Shimadzu HPLC system (Shimadzu, Japan), Hitachi LaChrom Elite HPLC System (Merck-Hitachi, Japan) and a Waters 2695 Alliance HPLC System with a PDA detector (USA). The mobile phase consisted of a mixture of 7 parts v/v of buffer (8.5 g/L of ammonium acetate, 1.25 g/L of cupric sulfate, pentahydrate, and 1.3 g/L of L-isoleucine in water) and 3 parts v/v of methanol with a column containing the L1 packing (Waters Symmetry C18 250 mm x 4.6 mm i.d. column, 5 μm particle size). The following conditions of separation were used: the oven temperature was 45 °C, the mobile phase flow rate of 0.8 mL/min (isocratic) and the injection volume was 25 µL. UV detection was carried out at 360 nm with the total running time of 26 min. The quantification method was based on a calibration curve using LV standard, in a concentration range from 5 μg/mL to 200 μg/mL (r^2=0.9999) Limits of detection and quantification were 1.97 μg/mL and 5.97 μg/mL, respectively. The same method was applied to run the standard of levofloxacin N-oxide (LNO) to identify its peak in both the raw material and the NLC formulations. For degradation analysis, the total amount of impurities, as percentage of area in the chromatograms, was considered and not only LNO. A normalization procedure based on the signal-to-noise ratio was used to determine the quantitation limit of impurities (Fig. S1).

Determination of total drug content, drug loading and entrapment efficiency (EE)

The determination of the total drug content was done by transferring 500 μL of the NLC suspension to a 50 mL volumetric flask, and then adding 1 mL of THF to partially dissolve the matrix. The resulting suspension was vortex mixed in a Quimis mixer, model Q220M (Brazil), for 2 minutes, to which 30 mL of the mobile phase was added, and the flask was sonicated in an ultrasonic bath for 5 minutes, with vigorous shaking every two minutes. After cooling down to room temperature, the volume of the liquid was made up to 50 mL in a volumetric flask, and the resulting solution was filtered through a PVDF membrane syringe filter Sartorius Minisart®, 25 mm in diameter and 0.45 μm pore size, discarding the first 2 mL of the filtrate.

EE was determined indirectly by the ultrafiltration method, using centrifugal filter tubes (Millex, Millipore, USA) with a 30 kDa molecular weight cut-off (Beraldo-de-Araújo et al., 2019). A volume of 500 μL of NLC suspensions were centrifuged at 4100 x g for 20 min in an Eppendorf 5418 centrifuge (Germany). Free LV in the supernatant was diluted 25x in the mobile phase and quantified according the HPLC method. EE was calculated based on the difference between the drug content in the formulations and the amount detected in the filtrate, applying Equation 1:

$$\text{EE}\ (\%) = \frac{\text{Total amount of drug} - \text{free drug}}{\text{Total amount of drug}} * 100 \quad (\text{Eq. 1})$$

Drug loading was calculated using Equation 2 (Papadimitriou and Bikiaris, 2009):

$$\text{DL}\ (\%) = \frac{\text{weight of entrapped drug in nanoparticles}}{\text{weight of nanoparticles (drug + excipients)}} * 100 \quad (\text{Eq. 2})$$

Formulation stability

The stability of the optimized formulation with and without LV was evaluated at pre-determined time points. The samples were stored in a stability chamber (40 °C and 75% RH) and parameters measured by DLS (z-average, PdI and zeta potential) in triplicate and results presented as mean ± standard deviation. Drug recovery, EE and total impurities were also evaluated by HPLC.

Dynamic vapor sorption (DVS)

First, 1 – 2 mL of the optimized nanosuspensions NLC_LV (with LV) and NLC_BL (blank, without LV) were poured into 20 mL open glass tubes. They were dried at room temperature inside a desiccator with silica gel for approximately 60 days before DVS studies. DVS analyses were performed using an Advantage-1 automated gravimetric vapor sorption analyzer (Surface Measurement Systems Ltd., UK) at 25.0±0.1 °C, with nitrogen as a dry carrier gas. Approximately 20 mg of the sample in the sample basket was placed in the instrument and equilibrated at 0% relative humidity (RH) overnight. The reference mass was recorded, and

sorption−desorption analysis was then carried out between 0 and 90% RH, in steps of 10% RH. At each stage, the sample mass was equilibrated (dm/dt ≤ 0.002 mg/min for at least 10 min and the maximum equilibration time was set as 480 min) before the RH was changed. An isotherm was calculated from the complete sorption and desorption profile (Mesallati et al., 2017). Water distribution within the samples was evaluated by Young-Nelson model as described previously (Mesallati et al., 2019).

Drug release profiles

Drug release was assessed by two methods, since there is no consensus about the most appropriate approach for nanoparticulates. Therefore, release studies were performed using Franz cells and carried out in 7 mL static vertical diffusion cells with automatic sampling (Microette Plus®, Hanson Research, USA). The receptor chamber was filled with PBS pH 7.4, covered with the cellulose membrane and the donor chamber was filled with 1 mL sample in PBS. The available diffusion surface area was 1.76 cm^2 and a clamp was used to hold the compartments together. Two diffusion cells were prepared for each sample tested. The receptor medium, maintained at 37 ± 1 ºC, was constantly mixed (magnetic stirring at 700 rpm), except during the periods of sample collection. Aliquots of 2.5 mL (with 1 mL accounting for purging and 1.5 mL used for analysis) were withdrawn at specific time intervals and collected into HPLC vials. The aliquots withdrawn from the receptor chamber were immediately replaced with the blank receptor medium at the same temperature. The LV concentrations were accordingly corrected considering the replenished volumes. The collected samples were analyzed by HPLC as already described above.

A non-membrane release method was adapted from (Magenheim et al., 1993) without the use of a membrane that separates the colloidal formulation from the release medium. The optimized LV-loaded NLC (100 µL) was poured into 2 mL-capped plastic tubes containing 900 µL of PBS 0.01 M pH = 7.4. The samples were placed in a shaking water bath (100 rpm, 37 °C) and every time point was run in quadruplicate. Every 0.08, 0.25, 0.5, 0.75 1.0, 1.5, 2, 2.5, 3, 4, 6 and 24 h, 500 µL of the samples were withdrawn and centrifuged immediately using 30 kDa Amicon centrifuge filters (4100 x g, 15 min, 21 °C). The supernatant was diluted 4x with the mobile phase and LV quantified by HPLC. There was one sample tube for each time point, avoiding the withdrawal of aliquots of LV together with nanoparticles from the samples and interfering with results of the next time points. Samples with the same concentration of free LV (0.5 mg/mL) were prepared by adding 20 mL of PBS into 10 mg of LV in 50 mL-capped plastic tubes at the same conditions as NLCs and analyzed by HPLC at the same time points to evaluate drug dissolution rate.

Statistical Analysis

Samples were evaluated as mean ± standard deviation. The statistical significance in the differences between samples was determined using a one-way analysis of variance (ANOVA). The differences were considered significant at $p < 0.05$. DoE analysis was made with the help of software Minitab® 17.1.0.

3. Results and discussion

3.1 Preformulation studies on NLC formulation components

We previously described the importance on evaluating critical formulation parameters (CQAs) to reach a good NLC, such as lipid type and amount, crystallinity and drug properties (Beraldo-de-Araújo et al., 2019). For this reason, we started with a preliminary visual evaluation of LV solubility in different lipids. The qualitative results are given in Table 1. It was expected that the lipids, in which LV dissolved better, can incorporate more the drug in the lipidic core (Bhalekar et al., 2017).

Table 1. Solubility of LV in lipids. ("-" did not dissolve; "±" partially dissolved; "+" completely dissolved).

Lipid type + Drug (%)	15 min	30 min	45 min	60 min
Beeswax + LV 1	-	±	±	±
Beeswax + LV 5	-	-	-	-
Dynasan 116 + LV 1	-	-	-	-
Dynasan 116 + LV 5	-	-	-	-
Gelucire 50/13 + LV 1	-	-	±	±
Gelucire 50/13 + LV 5	-	-	-	-
Geleol mono and diglycerides + LV 1	-	±	+	+
Geleol mono and diglycerides + LV 5	-	-	±	±
Cetyl Palmitate + LV 1	-	-	±	±
Cetyl Palmitate + LV 5	-	-	-	-
Precirol® ATO 5 + LV 1	+	+	+	+
Precirol® ATO 5 + LV 2.5	±	+	+	+
Precirol® ATO 5 + LV 5	-	-	±	±
Tego care 450 (Stearyl glucoside) + LV 1	-	-	-	±
Tego care 450 (Stearyl glucoside) + LV 5	-	-	-	-
Dynasan 118 + LV 1	-	±	±	±
Dynasan 118 + LV 5	-	-	±	±
Biogapress vegetal BM297 ATO + LV 1	-	+	+	+
Biogapress vegetal BM297 ATO + LV 5	-	-	±	±
Compritol® 888 ATO + LV 1	±	+	+	+
Compritol® 888 ATO + LV 5	-	±	±	±
Stearic acid + LV 1	+	+	+	+
Stearic acid + LV 5	-	-	-	-
Oleic acid + LV 1	±	+	+	+
Oleic acid + LV 5	-	±	±	±

It was noticed that LV at the higher loading (5% w/w) was not completely soluble at any of the lipids, with incomplete solubilization in Geleol, Precirol, Dynasan, Biogapress, Compritol and oleic acid, typically achieved after at least of 30 minutes of thermal treatment. However, LV, at 1% w/w level, dissolved entirely in Precirol and stearic acid after 15 min, followed by Compritol and oleic acid, with a partial solubilization at the same time point, but a complete dissolution after 30 min, as well as Biogapress. As the other lipids did not dissolve LV completely, they were therefore not included in further studies going forward. Since this test allows us to predict the success of drug incorporated in lipid carriers, we considered that it would be better to embedded LV in the lipids that solubilized the drug the most. Therefore, we have decided to prepare nanostructured lipid carriers (NLCs) with Precirol and/or stearic acid as solid lipids, and oleic acid as a liquid lipid. Compritol was dismissed because of its high melting point, which could impair the production by the proposed method, due to evaporation of the aqueous phase.

Thermal properties of the bulk ingredients and physical mixtures of excipients with 5% LV were determined using DSC and TGA (Fig. 1A and B). Since the chosen method of NLC production involves heat, we also evaluated the binary mixtures with thermal treatment at the condition of NLC production (58 °C, 30 min).

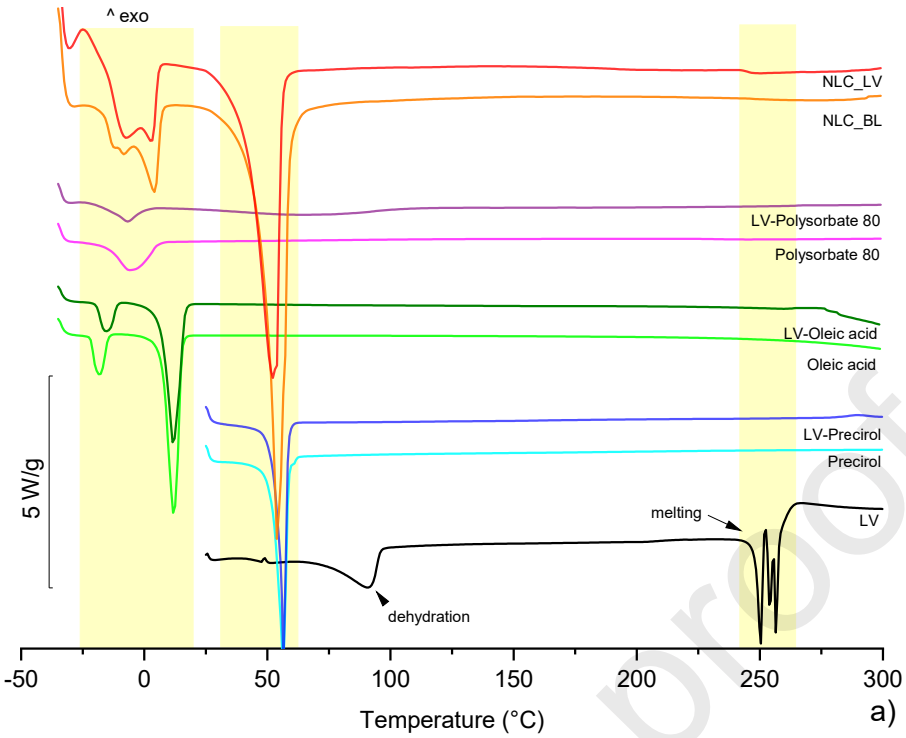

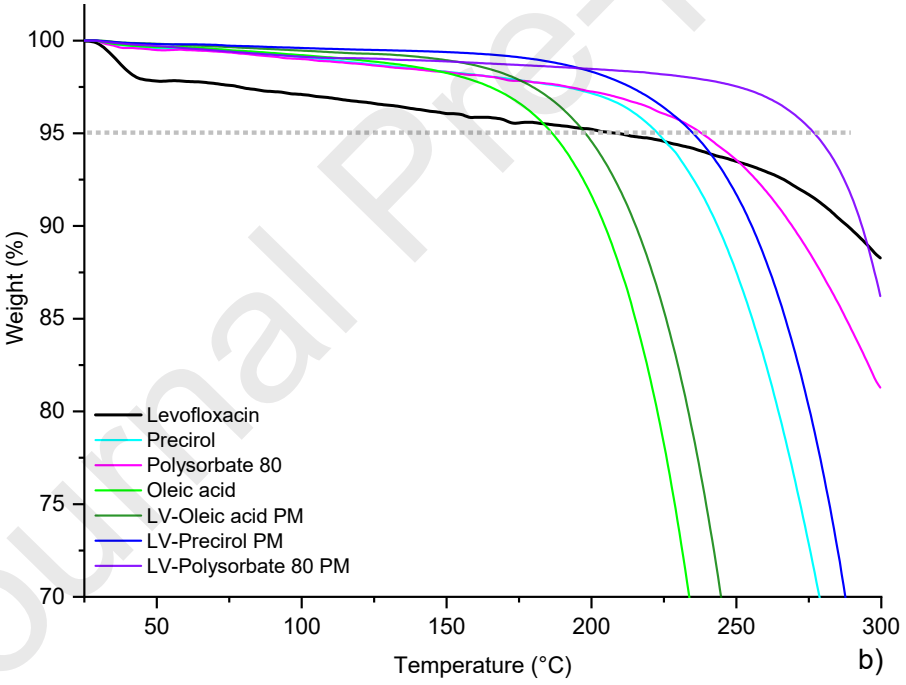

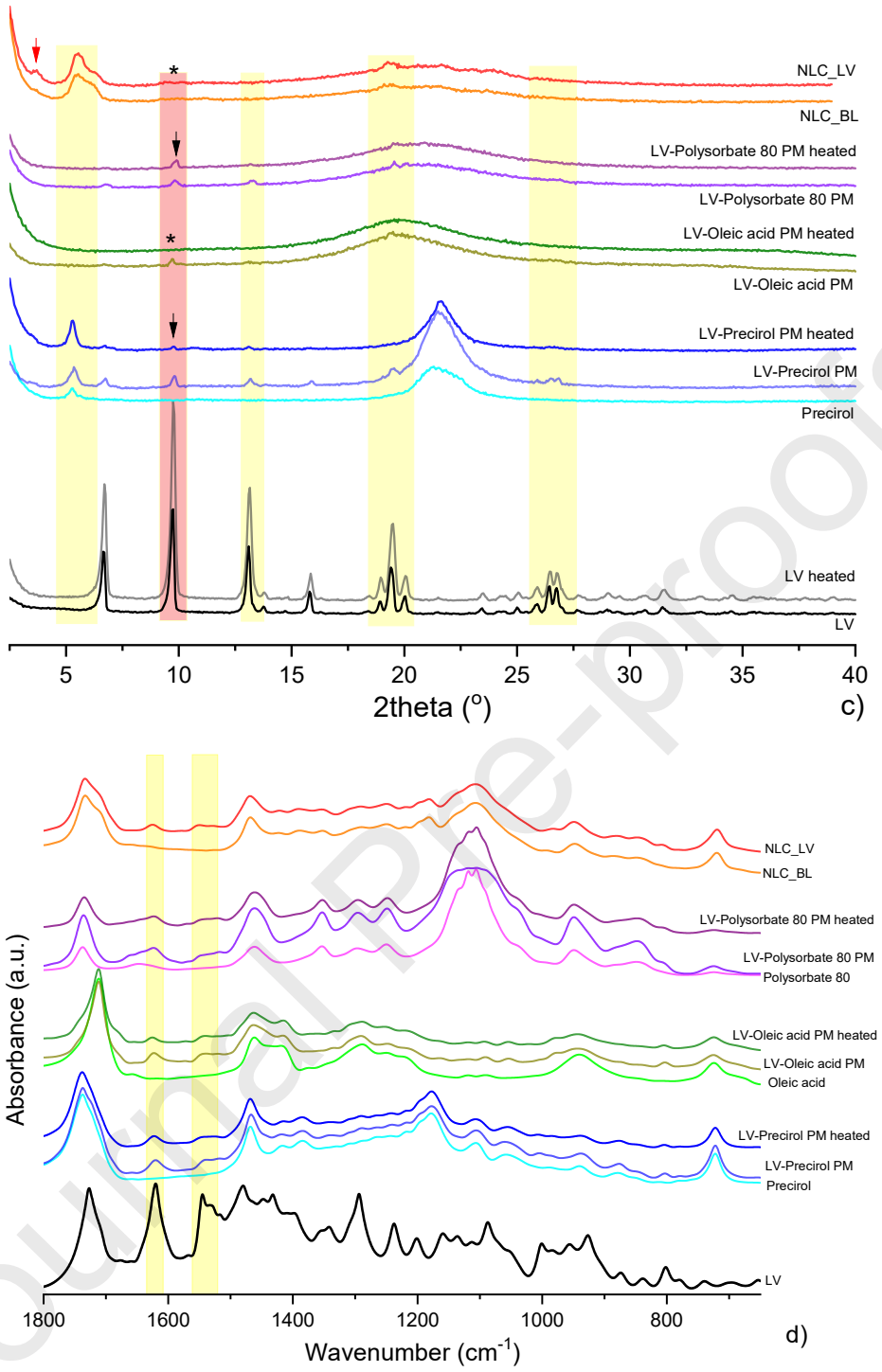

Figure 1. DSC (A), TGA (B), XRD (C) and FTIR (D) data of levofloxacin (LV), the chosen excipients to produce NLCs and their mixtures (5% LV + excipient), at room temperature or after thermal treatment (58 °C, 30 min), and the optimized NLC with and without LV (NLC_LV and NLC_BL, respectively). Yellow rectangles indicate areas characteristic of LV and/or excipients (DSC). Black arrows indicate the presence of LV and stars disappearance of the LV Bragg peak in the heated samples; the red arrow shows the peak position suggesting a liquid crystalline arrangement of the NPs (XRD).

TGA presents decomposition of the samples on heating. Clearly, oleic acid and its mixture with LV have the lower decomposition temperatures, starting at 195-200 °C and being the

least thermally stable mixtures (Fig. 1B and Table 2). Degradation also appears in the DSC mixture LV-oleic acid (~275 °C, Fig. 1A). All the physical mixtures have the onset of the decomposition temperature (at 5% weight loss) higher than for the ingredients alone.

DSC thermograms present the melting points of each component in accordance with the literature (Table 2). Specifically, LV has an endothermic transition due to dehydration with an onset at 48.6 °C and a broad temperature range (40-75 °C) (Fig. 1A). It can also be seen in TGA (~3% weight loss until 50-55 °C, in agreement with the stoichiometric amount of water loss in hemihydrate LV molecules, 2.43% w/w) (Gorman et al., 2012) (Fig. 1B). Melting, at app. 224.6 °C, followed by extensive decomposition was then observed, with a possible underlying polymorphic transformation (Gorman et al., 2012; Nisar et al., 2020). XRD analysis showed that LV hemihydrate was crystalline in accordance with literature (Wei et al., 2019) and it maintained crystallinity after heating (Fig. 1C).

Precirol presents only one endothermic melting event at 51.6 °C (Table 2) in agreement with the values published before (Hamdani et al., 2003). The same transition occurred in both pure sample and mixture with LV 5% (Fig. 1A), but no event due to LV melting, was found, suggesting that LV may dissolved in the lipid matrix (Abdel Hady et al., 2020). XRD presented that Precirol had a semi-crystalline structure with a Bragg peak at app. 5.3 °2θ and a broad "halo" between 20-23 °2θ. The diffractogram of the physical mixture of this excipient with 5% w/w LV displayed weak intensity peaks characteristic of the drug, which reduced in intensity following heating to 58 °C and cooling to RT. Thus, LV partially dissolved in this lipid as expected from the qualitative solubility studies. Oleic acid had two endothermic events, corresponding to the solid–solid transition from γ to α form (-21.9 °C) and then the α form melting (7.0 °C). The solid-solid transition temperature is lower than that found in the literature for pure and dry oleic acid (between -3 to -5.7 and 12.2 to 13 °C, respectively) (Inoue et al., 2004; Wartewig et al., 1998), maybe because we used the super refined grade of this excipient. Mixing oleic acid with LV 5% did not change its transitions on heating and no LV melting event was seen, suggesting that the drug dissolved in the liquid (Fig. 1A). XRD confirmed that oleic acid was a good solvent for LV, as no peaks of the drug were seen in the mixtures that was heated and then cooled to RT (Fig. 1C). LV at this concentration was detected by XRD as seen for the Precirol system. Polysorbate 80 presented a broad melting range temperature with an onset at -15.4 °C and a broader event when mixed with 5% LV starting at 17.0 °C, which could be dehydration. Again, no peaks of LV were found. From XRD analysis, we can conclude that the LV did not completely dissolve in the surfactant, but there was evidence of partial solubility (Fig. 1C).

Table 2. Thermal characterization of levofloxacin (LV), the excipients, physical mixtures and optimized NLC (placebo and with LV). Degradation temperature is the temperature at which up to 5% weigh loss occurred.

		DSC		
Ingredient	**Degradation temperature (°C)**	**T_{Onset} (°C)**	**ΔH normalized (J/g)**	**Probable event**
Levofloxacin	145-150	48.6	-76.4	dehydration[1]
		224.6	N/A	γ form melting[1]
		229.5	N/A	β form melting[1]
		232.3	N/A	α form melting[1]
Precirol	220-225	51.6	-137.4	melting[2]
Oleic acid	185-190	-21.9	-27.1	γ to α polymorph[3]
		7.0	-135.6	α form melting[3]
Polysorbate 80	235-240	-15.4	-57.2	
		225.8	-3.2	
LV-Precirol	235-240	54.2	-122.6	Precirol melting
		282.0	2.9	possible LV degradation
LV-Oleic acid	195-200	-19,5	-24.0	γ to α polymorph
		6,6	-126.9	
LV-Polysorbate 80	275-280	-16.2	-23.8	
		17.0	-53.9	
NLC_LV (dried at RT)	190-195	-20.9	-39.2	
		41.2	-80.7	Precirol melting
NLC_BL (dried at RT)	190-195	-6.7	-29.2	
		48.9	-102.5	Precirol melting

* Events based on the literature reports: [1] from (Kitaoka et al., 1995); [2] from (Jannin et al., 2006); [3] from (Inoue et al., 2004)

Supporting thermal analysis and XRD studies, IR clearly showed the presence of LV in the mixtures with excipients. The most characteristic were stretching vibrations of the ring carbonyl group ν(C=O) at 1620 cm^{-1} and ν(C=C) of the ring at 1541 cm^{-1}. These principal LV absorptions shifted slightly following heating with oleic acid and Polysorbate 80, to 1623 and 1539 cm^{-1} as well as 1624 and 1550 cm^{-1}, respectively, with larger deviations seen for the mix with Polysorbate 80. It could suggest weak intermolecular interactions between the components. There were no band shifts for LV in Precirol. Collectively, based on the above studies, LV showed the ability of not only solubilize in the selected excipients, but also to interact with them at molecular level, potentially affecting the NLC formation and their structure. This finding is supported by the work of Ortiz-Collazos et al. showing that LV was able to increase the thickness of the acyl tails in 1,2-dipalmitoyl-sn-glycero-3-phosphocholine monolayers (Ortiz-Collazos et al., 2019). A related molecule, ciprofloxacin, has been asserted to interact with oleic acid via ionic chemical interactions and/or hydrogen bonds (Torge et al., 2017). As a result of preformulation studies presented in this section, the key CMAs were determined.

3.2 Optimization of NLCs

Based on our previous experience and reports published by other groups (Beraldo-de-Araújo et al., 2019; Ferreira et al., 2015; Hejri et al., 2013; Kelidari et al., 2017; Subramaniam et al., 2020), optimization of the NLC process and formulation aspects was carried out. Several attributes were investigated: the key excipients and their proportion as well as the process parameters. Following on preformulation studies, pilot NLCs were fabricated with Precirol and stearic acid as prospective solid lipids and oleic acid as a liquid lipid. While both preliminary NLCs showed good LV incorporation and parameters (NLC with stearic acid: 589 ± 22 nm mean particle size, PdI 0.32 ± 0.01, EE 62%; NLC with Precirol: 180 ± 30 nm mean size, PdI 0.23 ± 0.03 and EE 57%), the formulation containing stearic acid became very viscous after 24 h, therefore this formulation prototype was excluded from further studies. A similar behavior was observed by Umerska and co-workers when the nanocapsules with stearic acid solidified after preparation (Umerska et al., 2016).

Having determined the NLC composition, a full factorial design of experiments 2^3 was performed to choose the proportion of excipients, which would ensure the optimum formulation in terms of physicochemical properties. The following targets were determined: z-average of around 200 nm, to avoid reticule-endothelial rejection (Martins et al., 2012; Wang et al., 2020), PdI ≤ 0.3 to reduce e.g. Ostwald ripening (Wooster et al., 2008), high absolute zeta potential values to ensure physical stability and high EE. The inputs (factors) for each of the formulations and the obtained responses are presented in Table 3. Theoretical drug loading (TDL) was also provided for comparisons.

Table 3. Full factorial 2^3 design of experiment with triplicate of the center point. TDL: theoretical drug loading. Factors: total lipids (TL), amount of surfactant (% w/v) and total proportion of solid lipid (SL) compared to liquid lipid (% w/w). Responses: z-average, polydispersity index (PdI), zeta potential (ZP, measured using milliQ water as the diluent) and EE.

Formulation composition			**Factors**			**Responses**			
Code	TDL (%)	Lipid/aqueous phase ratio (g/g)	TL (mg)	Surfactant (% w/v)	Total SL (% w/w)	z-average (nm)	PdI	ZP (mV)	EE (%)
S1	3.86	0.5/10	500	2	70_30	144 ± 2	0.238 ± 0.008	-40 ± 0.7	73.3
S2	2.95	1/10	1000	2	70_30	199 ± 4	0.317 ± 0.025	-44 ± 1	85.6
S3	2.99	0.5/10	500	4	70_30	71 ± 3	0.368 ± 0.067	-43 ± 4	56.8
S4	2.76	1/10	1000	4	70_30	162 ± 0.3	0.242 ± 0.008	-40 ± 0.8	80.1
S5	2.21	0.5/10	500	2	90_10	126 ± 0.4	0.202 ± 0.013	-42 ± 2	41.9
S6	2.27	1/10	1000	2	90_10	234 ± 1	0.288 ± 0.036	-41 ± 2	65.9
S7	1.23	0.5/10	500	4	90_10	87 ± 0.6	0.207 ± 0.003	-31 ± 1.1	23.3

S8	2.28	1/10	1000	4	90_10	143 ± 0.6	0.242 ± 0.002	-38 ± 0.7	66.2
S9_1	2.50	0.75/10	750	3	80_20	152 ± 2	0.210 ± 0.011	-40 ± 0.7	59.9
S9_2	2.86	0.75/10	750	3	80_20	141 ± 0.6	0.222 ± 0.002	-42 ± 0.5	68.7
S9_3	2.70	0.75/10	750	3	80_20	150 ± 1	0.260 ± 0.036	-41 ± 2	64.7

The linear model provided a good explanation of the z-average parameter (r^2=0.996). The contour z-average plot (Fig. 2A) shows the positive and negative influence of TL and surfactant, respectively, on nanoparticle size indicating that the higher amount of TL and the lower amount of surfactant, the greater nanoparticle size. Pareto charts show that TL has a significant influence on z-average (Fig. 2E), which is reasonable, because of the abundant availability of excipients in the formulation, which allows the constitution of bigger nanoparticles (Das et al., 2011; Martins et al., 2012). On the other hand, the amount of surfactant has a negative influence, which means that the highest the surfactant concentration, the smaller nanoparticle size (Martins et al., 2012). This may be due to the coating effect of the surfactant, as the more surfactant available, the more lipid nanodroplets would be coated and be smaller and/or lowering surface tension.

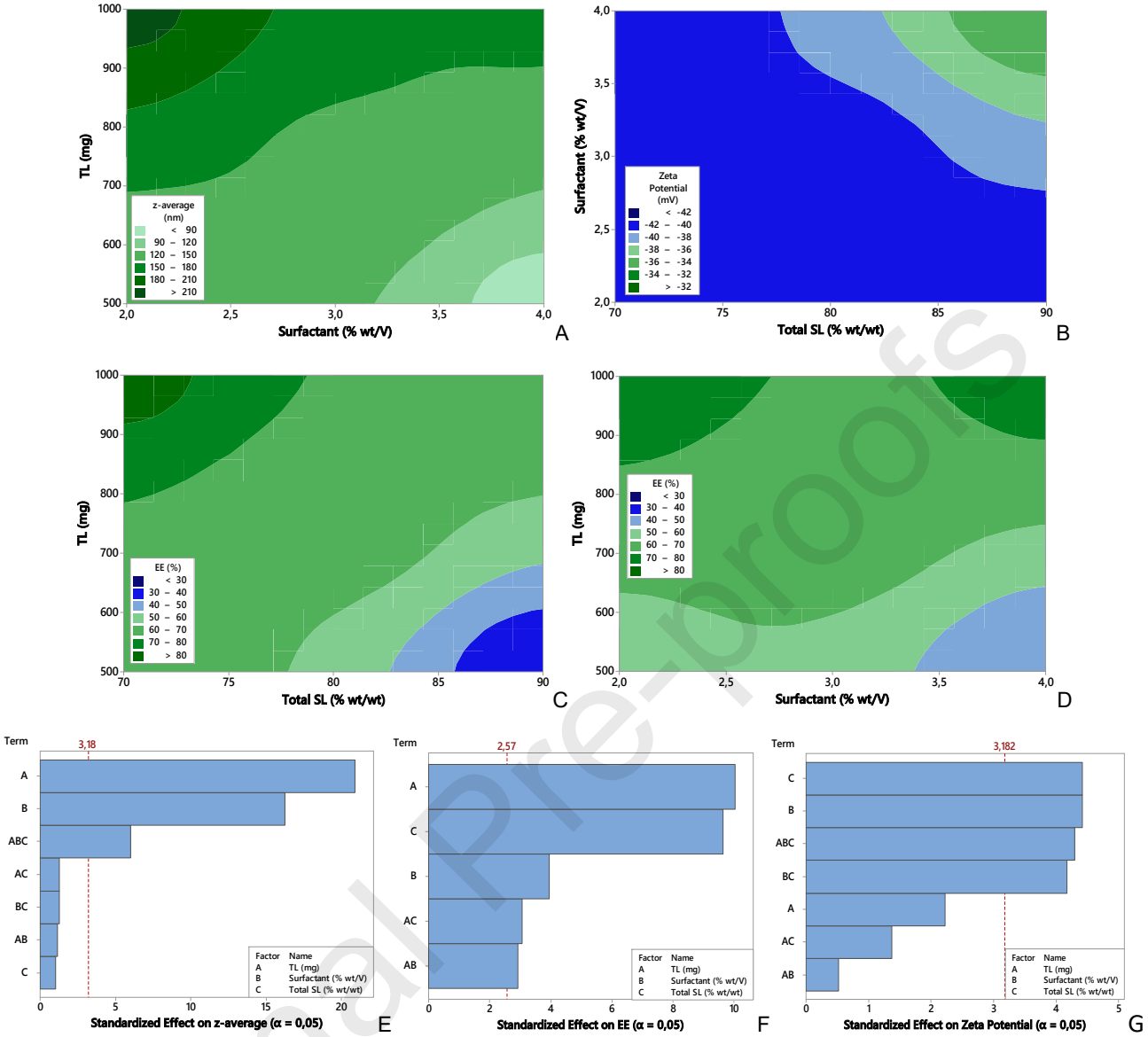

Figure 2. Contour plots (A-D) and Pareto charts (E-G) with outputs under the significant influence of DoE factors (α = 0.05). The contour plots illustrate how two factors may affected the outputs (z-average (A), zeta potential (B) and EE (C and D)). Pareto charts show the factors that have influenced the outputs (bars that exceed the threshold red lines for z-average (E), EE (F) and zeta potential (G).

Determination of zeta potential depends on the surface charge and it is important when comes to predicting the colloidal stability of nanoparticles in a suspension (Rasmussen et al., 2020). This response was influenced by all the factors in the DoE (r^2=0.9647), except by TL alone (Fig. 2B and 2G). The difference in the total amount of lipids did not change, on its own, the surface charge of nanoparticles, which occurred when we varied the concentrations of each excipient. To illustrate, Fig. 2B presents that the increased amount of total SL and surfactant lead to an increase in zeta potential (less negative). On the other hand, the interaction of the

three factors has a negative effect, resulting on the zeta potential values being more negative. There was no factor with a significant influence on PdI.

Finally, an increasing amount of TL resulted in an increase in EE (Fig. 2C, 2D, 2F), most likely due to greater amount of lipids able to entrap more LV (Das et al., 2011). But increasing the quantity of solid lipid had the opposite impact, the EE values decreased, most likely because LV has more affinity to the liquid lipid, as suggested by DSC, XRD and FTIR results (Fig. 1 A, C and D, respectively). When there was more liquid lipid (30% of LL) in the formulation, more LV got incorporated in the NLCs and with lower quantities of LL (10%), lower EE values were obtained. The surfactant led to a decrease in EE, probably because it increased LV solubility in the aqueous phase. However, at the higher amounts of TL, the higher concentration of surfactant did not affect the EE (r^2=0.9784).

The formulation S1 presented the highest theoretical drug loading (3.86%, Table 3), but its EE was not the highest, as expected for formulations with a low TL level. On the other hand, S2 had the highest EE, but solidified on storage, perhaps due to its low level of surfactant (2%). For these reasons, the subsequent experiments with performed using the composition of the formulation S4 due to its high EE (high levels of TL and the liquid lipid) and the physical stability of the dispersion (high surfactant concentration, 4%). Preliminary stability tests on the S4 dispersion carried out at room temperature showed that this system was stable for 15 days. The formulation on day 15 had the following characteristics: z-average 176 ± 2 nm; PdI 0.188 ± 0.010; zeta potential -44.8 ± 0.7 mV, and no visual changes in viscosity or homogeneity were noticed. A replicate was produced, and its zeta potential was evaluated after dilution in 10 mM NaCl instead of milliQ water. The change of the dilution medium was introduced as it is more physiological than ultrapure water. This protocol changed the zeta potential value of the samples from around -40 to nearly -20 mV, expected due to screening of the surface charge by NaCl (Skoglund et al., 2017).

The initial process parameters used in the above DoE were based on our previous experiments (Beraldo-de-Araújo et al., 2019) (30 minutes of sonication at 50% amplitude) and selecting the process temperature of 58 °C to ensure full melting of the solid lipid. However, after optimizing the proportion of excipients to ensure the best physicochemical properties of LV formulation, we discovered an indication of drug degradation, of around 4% of total impurities, when performing HPLC analysis for EE. Since the limit of total impurities for LV according to United States Pharmacopeia is 0.5% (“Levofloxacin,” 2017), a new full factorial 2^3 design was designed and performed, introducing process variations to improve NPs with acceptable values of total impurities (Table 4). The analytical grade oleic acid was replaced by Super Refined™ oleic acid, as this change was related with the decrease of LV impurities,

mainly LNO, in further tests of LV-excipients compatibility (data not shown). The level of peroxides in pharmaceutical excipients has been known to affect the purity levels of drugs, such as disulfiram (Chen et al., 2015) and others (Khanum and Thevanayagam, 2017).

Table 4. Full factorial 2^3 design of experiment with triplicate in center point, containing the inputs: temperature (T), sonication time and sonication amplitude. TDL: Theoretical drug loading. The outputs are z-average (measured using 10 mM NaCl as the diluent), polydispersity index (PdI), zeta potential (ZP), entrapment efficiency (EE) and total impurities (SD = standard deviation; n = 3).

Formulation		Factors			Responses				
Formulation #	**TDL (%)**	**T (°C)**	**Sonic. time (min)**	**Sonic. amplitude (%)**	**z-average ± SD (nm)**	**PdI ± SD**	**ZP ± SD (mV)**	**EE (%)**	**Total impurities (%)**
F1	3.48	38	10	30	168 ± 2	0.317 ± 0.036	-24 ± 0.8	75.9	0.37
F2	3.46	78	10	30	183 ± 4	0.353 ± 0.033	-22 ± 0.8	77.5	0.75
F3	3.51	38	30	30	156 ± 3	0.271 ± 0.01	-24 ± 1	75.5	0.43
F4	3.48	78	30	30	169 ± 6	0.322 ± 0.029	-24 ± 0.9	75.4	1.09
F5	3.47	38	10	70	138 ± 1	0.266 ± 0.025	-21 ± 0.7	73.9	0.56
F6	3.42	78	10	70	163 ± 1	0.256 ± 0.007	-22 ± 1	72.2	0.74
F7	3.52	38	30	70	132 ± 1	0.227 ± 0.017	-21 ± 0.7	74.7	0.53
F8	3.47	78	30	70	164 ± 1	0.267 ± 0.006	-21 ± 0.4	78.9	1.13
F9_1	3.49	58	20	50	140 ± 2	0.238 ± 0.007	-21 ± 0.4	77.7	0.48
F9_2	3.43	58	20	50	138 ± 2	0.247 ± 0.005	-21 ± 0.8	71.9	0.53
F9_3	3.45	58	20	50	142 ± 0.2	0.281 ± 0.032	-21 ± 0.6	75.2	0.63

After analyzing the outcomes, we were able to determine that temperature and sonication amplitude had the most impact on the z-average values, with the highest values of temperature resulting in larger NP sizes, while the highest amplitude gave smaller NP sizes, followed by the sonication time (longer sonication gave smaller nanoparticles) (r^2 = 0.9917) (Fig. 3A). The sonication amplitude was the only factor affecting PdI (lower PdI values were obtained with higher sonication amplitude, r^2 = 0.5072) (Fig. 3B). Zeta potential appeared to be dependent on a multitude of factors and their interactions (r^2 = 1), but, from a practical point of view, the values of zeta potential were all acceptable (around -20 mV) and, in addition, polysorbate 80 is a nonionic surfactant providing steric stabilization to the nanoparticles. The backward elimination (α = 0.05) removed all terms from the model pertaining to EE, thus it was not possible to determine the significant factors impacting the EE values. Importantly, the highest content of total impurities was related to the highest levels of temperature and sonication time (r^2 = 0.9641) (Fig. 3D).

Regarding the process parameters, we focused on total impurities and PdI, since all the particle size values were < 200 nm, zeta potential below -20 mV and EE was not statistically influenced by any DoE factor. Therefore, it was decided to avoid the highest temperature and longest sonication time to prevent LV degradation. However, working with these two parameters at the lowest levels lead to formulations with higher apparent viscosity, thus it was decided to work with their intermediate levels (58 °C and 20 min, respectively). As there was a weak correlation (r^2= 0.5072) between high amplitude of sonication and low PdI, then this value was fixed it at 50%. In summary, the only change introduced to the process conditions was the duration of the sonication process, reduced from 30 to 20 minutes.

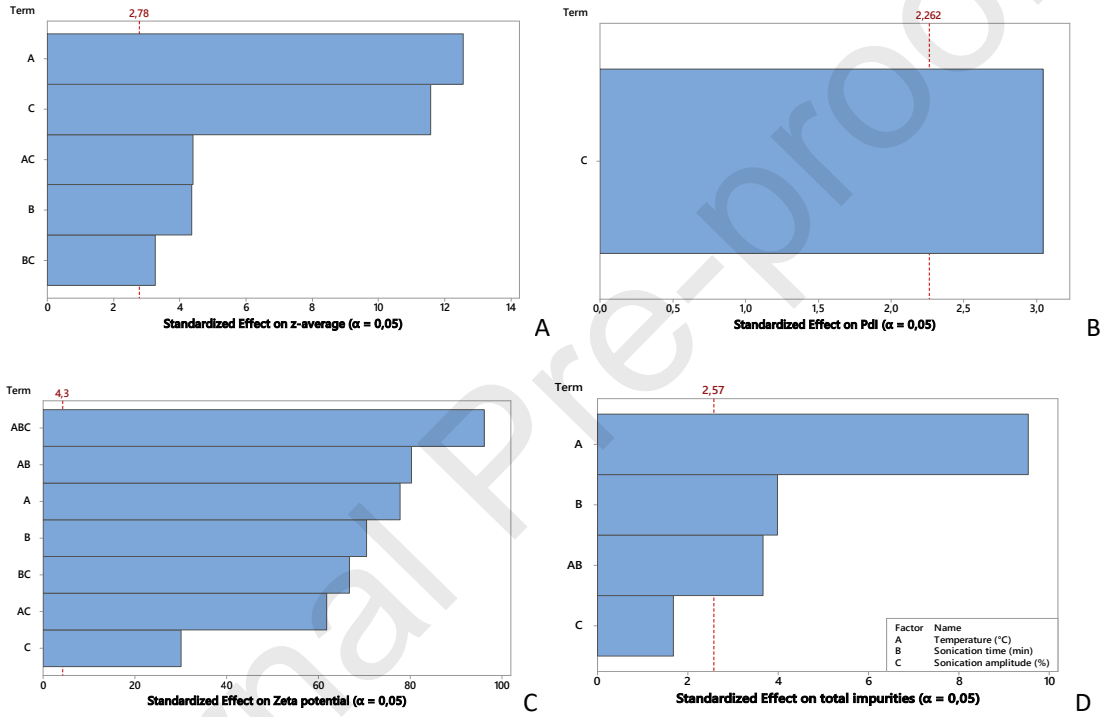

Figure 3. Pareto charts of the effect of the factors on the dependent variables z-average (A), PdI (B), zeta potential (C) and total impurities (D). The bars correspond to the factors or their interactions. The bars that surpassed the Bonferroni limits have a relevant interference on the respective outputs.

Overall, superior formulations were designed as guided by the DoEs, with greater EE values than those published for lipid nanocarriers. There is only one account that reports on the maximum of entrapped LV of ~ 56% that could be incorporated in NLCs (Islan et al., 2016). Another study loaded almost the same amount of LV on solid lipid nanoparticles (SLN) as that reported in the Islan et al. study (Islan et al., 2016), however, SLNs are known as not an optimum option for an entrapped drug in terms of the long term stability (Abdel Hady et al., 2020). Polymeric nanoparticles were the most chosen carriers to deliver LV, including the

PLGA-based systems. The success in terms of obtaining high EE values seems to depend on the type of polymer and the method of nanoparticle production, and could reach between ~ 3% with chitosan (Ameeduzzafar et al., 2018) and ~ 91% with PLGA (Shah et al., 2020). Although polymeric and lipid nanoparticles have been applied to carry LV, the natural and biological source of lipids yield nanoparticles potentially less toxic than polymeric NPs, depending on the polymer (natural, semisynthetic or synthetic origin), and easier to scale up (Müller et al., 2000; Rezigue, 2020).

3.3 Solid state properties of optimized NLCs

Following the optimization of the composition and process condition, thermal properties of the LV loaded NLC (NLC_LV) were compared to the unloaded carrier equivalent (NLC_BL). The thermograms of both were comparable, showing a range of endothermal peaks up to 25 °C, as the ones of oleic acid and Polysorbate 80. The melting peaks of Precirol were broader and shifted to lower temperatures, being affected by the liquid oleic acid and Polysorbate 80 (highlighted on Fig. 1A). In addition, a very low intensity endotherm at around 250 °C was noted for NLC_LV, most likely of LV. The heating improved LV solubilization in the excipient mixture, and in the optimized NLC_LV one could see the presence of a faint crystalline LV peak at ~18-20° 2θ that may be due to the non-solubilized drug (Fig. 1(c)). This peak was absent in NLC_BL. This is in accordance with the further EE determination and the presence of ~25% free LV (Table 3). Interestingly, in both NLC samples an extra, low intensity peak was seen at 3.7° 2θ, absent from diffraction patterns of the components and it was not caused by a polymorphic transformation of LV occurring on heating. It might be due to the liquid crystalline arrangements of NLC components and this periodicity was estimated to be approximately 2 nm (Nonomura et al., 2009).

The partial solubility of LV in the NLC mixture along with the possible intriguing lamellar structure of the NLC prompted further investigations by DVS. The isotherm plots of NLC_LV and NLC_BL were similar (Fig. 4 A). The desorption data followed sorption data. At the end of the sorption cycle both NLC_LV and NLC_BL sorbed the same amount of water (approximately 9%). At the end of the desorption cycle, the mass was similar to the initial mass (change in mass was smaller than 0.05%). Both samples sorbed approximately 5.7% of water at 80% RH, so they can be considered as moderately hygroscopic, considering their lipidic constitution (2-15% w/w of water uptake at 25 °C/80 RH, (Newman et al., 2008)).

The only difference between the loaded and unloaded NLCs was seen in the kinetic DVS plots (Fig. 4B), indicating that after exposure to 0-90% RH at all RH steps the equilibrium was established, and that moisture sorption and desorption occurred rapidly at low RH and became slower at higher RH (80-90%). The incorporation of LV shortened both, sorption and

desorption cycles: the sorption cycle lasted approximately 13 hours and 15.5 hours for NLC_LV and NLC_BL, respectively, whereas the completion of both, sorption and desorption cycles (0-90-0% RH) took approximately 23.5 and 28.5 hours, respectively.

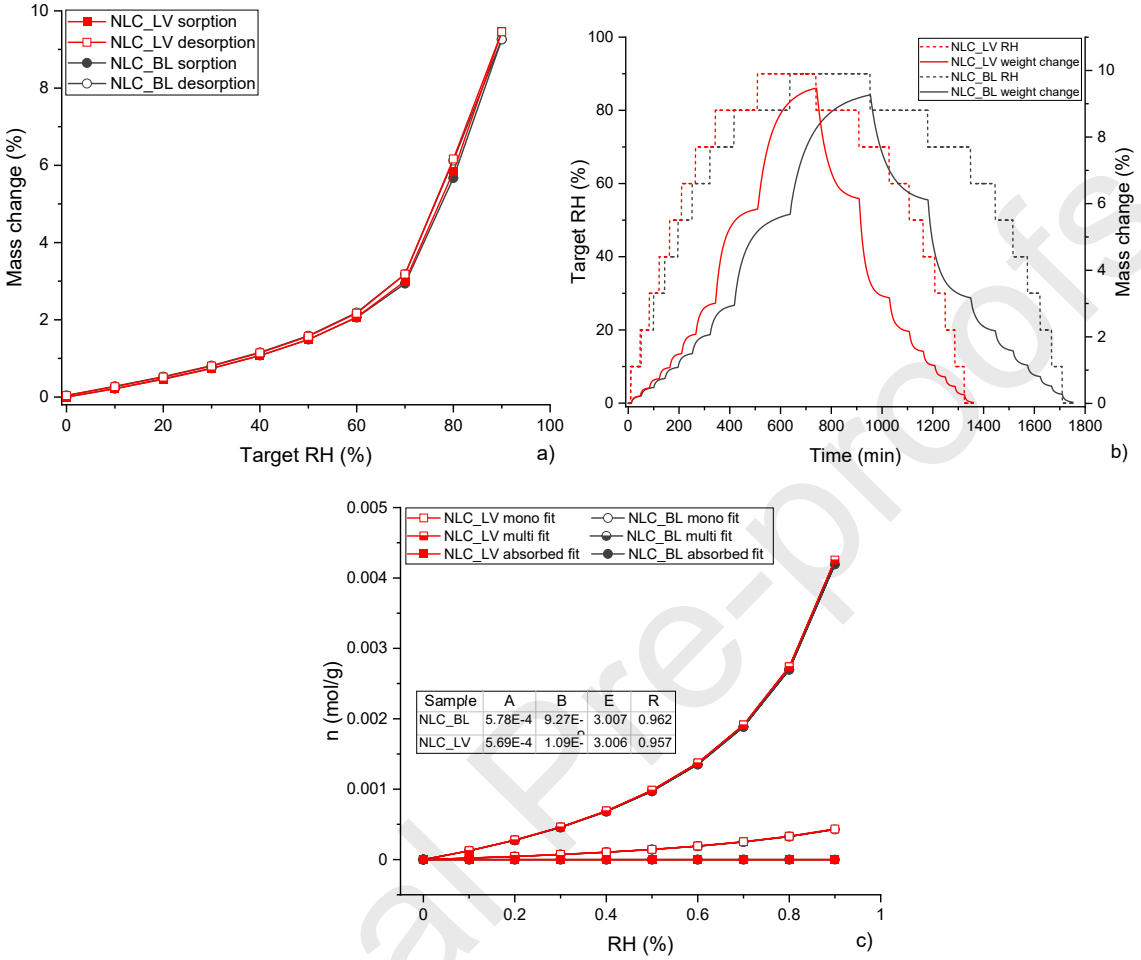

Figure 4. (A) Moisture sorption and desorption isotherm plots of NLCs at 25 °C, (B) Moisture sorption and desorption kinetic plots of NLCs at 25 °C. Broken lines show RH variations during sorption (0 – 90% RH) and desorption (90 – 0% RH), while solid lines show mass change (%) during the same conditions of sorption and desorption, (C) Water distribution patterns according to the Young-Nelson model in NLCs (mono fit refers to a monomolecular adsorption layer; multi fit refers to an adsorption as a multilayer and adsorbed fit refers to adsorption into the interior of nanoparticles) with parameters estimated from the Young-Nelson model for dried NLCs presented in the table: A - fraction of adsorbed water (mol/g), B - fraction of absorbed water (mol/g), E - Young-Nelson equilibrium constant, R: regression coefficient. NLC_BL: blank lipid NPs and NLC_LV: levofloxacin-loaded lipid NPs.

Considering the very similar isotherms for NLC_LV and NLC_BL, it was of no surprise that the water distribution patterns, according to the Young-Nelson model (Mesallati et al., 2019), were also alike (Fig. 4C). According to this model, water can be taken up by a sample in three different ways: adsorbed as a monomolecular layer, adsorbed as a multilayer, or absorbed

into the interior of the sample (James H. Young and G. L. Nelson, 1967). Most water taken up by the NLCs was bound to their exterior surfaces as a multilayer (Fig. 4C). A small part of water taken up by the particles was adsorbed as a monolayer. The water did not penetrate to the interior of the nanoparticles, as reflected by the value of fraction of absorbed water, which was 4-5 orders of magnitude lower than the fraction of adsorbed water (Fig. 4C). This is consistent with the hydrophobic nature of the NLC core, which does not allow water penetration.

Therefore, this analysis showed that NLCs has a lipidic core with part of LV solubilized in this lipidic core, while the outside possibly had a more hydrophilic, lamellar-like construction with the remaining LV molecules dispersed throughout.

3.4 Drug release

The dissolution of free LV was carried out for 24 h and compared to the drug release profile from NLC_LV at the same conditions (Fig. 5). The free LV had a fast and complete dissolution in the PBS medium, as expected of a class I BCS drug (high solubility and high permeability) (Koeppe et al., 2011). Around 85% of the entrapped drug released after 15 min with the remaining LV amount contained in the nanoparticles within the timeframe of the experiment (24 h). The entrapped LV may be bound to the lipids, as hypothesized above, since no degradation was detected by HPLC. We also performed a release experiment using the Franz cell apparatus, which has a cellulose membrane separating the donor from the acceptor compartments. Free LV presented a slow permeation rate through the membrane with a longer release time when compared to the results of the test with no membrane. The drug from NLC_LV had a delayed release profile in the Franz cell method when compared to the free drug in the same setup, resulting in nearly 50% release after 5 h. At the end of the test, approximately 10% was also retained in NLC.

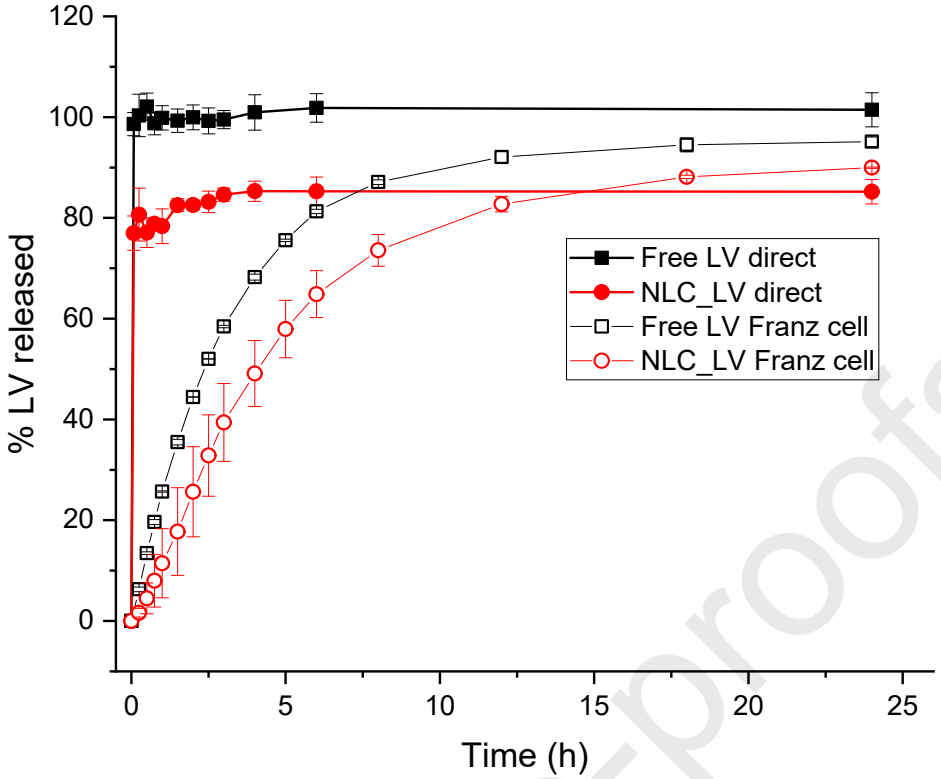

Figure 5. LV release profiles. Free LV dissolution (black filled squares, n=4), LV from NLC_LV using the direct method (red filled circles, n=4), free LV in the Franz cell apparatus (black open squares, n=2) and LV from NLC_LV in the Franz cell apparatus (red open circles, n=2), The medium in the direct method and the acceptor compartment in the Franz cell method was PBS 0.1 M, pH 7.4.

Abdel Hady and co-workers incorporated LV and doxycycline in SLNs and performed drug release by the dialysis bag method (Abdel Hady et al., 2020). They found that 50% of LV released after 5 h from the SLN with the intermediate amount of surfactant (2.125% of Span 60), which is in line with our results. Other researchers produced NLCs of LV with DNAse and also assessed the release profile by the dialysis method. They found nearly 60% release after 5 h, close to our results, at the same timepoint (Islan et al., 2016). Noteworthy, both studies did not present the corresponding release profiles of free LV, therefore we cannot compare the differences in the LV permeation rate based on the literature data.

The rapid LV release from NLC_LV upon direct dilution in PBS could indicate a fast release in an intravenous application. In contrast, the cellulose membrane studies showed a slower release. The membrane test is closer to a mucosal application, such as nasal and pulmonary routes of administration, where the local fluids have a small volume suggesting that these NLCs with modified release might be valuable for LV administration on mucosal surfaces. In addition, the non-released amount of LV from the NLCs corresponds to approximately 400

μg/mL, which is sufficient to inhibit bacteria that are susceptible to this drug (Grillon et al., 2016). Since NLCs have been shown to enhance internalization of several drugs (Barbosa et al., 2016; Garbuzenko et al., 2019) and LV has a limited efficacy of intracellular bacterial killing (Nguyen et al., 2006), our formulation has potential to enhance LV activity against intracellular bacteria, regardless of the administration route.

3.5 Accelerated stability test

Accelerated stability tests with both free and LV-loaded optimized samples (NLC_LV and NLC_BL) were performed. The samples were kept in a stability chamber for 30 days at 40 °C and 75% RH, which might correspond to 4 months of long-term stability, according to the Arrhenius equation (Nicoletti et al., 2009). The parameters evaluated before and after the incubation were z-average, PdI, zeta potential, EE, drug recovery and total impurities.

NLC_BL increases in size and PdI, followed by an increase in zeta potential. After 30 days of incubation, the apparent viscosity considerably increased, probably related to the strength of the interfacial film (Fang et al., 2008). On the other hand, NLC_LV presented acceptable physical stability, keeping the size constant between 138 and 145 nm, which is in a range required to avoid reticule-endothelial rejection (100-300 nm) (Wang et al., 2020). The PdI (0.241-0.223) and zeta potential (-18.1 to -15.9 mV) values presented slight fluctuations which did not impact on the stability or the formulation dispersity. The particles in the mentioned size range and negatively charged are adequate, for example, for a pulmonary route of administration, being able to penetrate lung mucus barrier (Finbloom et al., 2020). EE and drug recovery values were also maintained (1.2% and 2% variation, respectively), while total impurities increased by a 1.7-fold in relation to the initial amount. But, as the greatest amount of impurities were detected outside the NPs (the filtrate), the carrier probably protected the incorporated drug from degradation.

These findings have shown the significance of performing formulation and process studies with a drug stability indicating method. To avoid LV degradation, NPs could be dried following the formulation process suing a secondary pharmaceutical process. The complexation of LV to cations could help to stabilize LV, as suggested by Brillaut et al., for another fluoroquinolone, ciprofloxacin, which resulted in decrease in drug permeability, a desirable feature for pulmonary administration and local action (Brillault et al., 2017). Noteworthy, Seedher and Agarwal reported that this complex with LV may reduce antibiotic activity due to altered albumin-binding rates, which should be considered when planning intravenous or oral administrations, but it would not be an issue to a non-systemic route of delivery such as pulmonary (Seedher and Agarwal, 2010). Thus, the incorporation of LV in NLC enhances drug stability, protects the drug from degradation and have adequate characteristics for various

routes of administration (Ghasemiyeh and Mohammadi-Samani, 2018; Thapa et al., 2021), including the inhalation route (Gelperina et al., 2005).

4. Conclusions

In this study, we investigated the CMAs for the levofloxacin lipid-based nanoparticles, selecting biodegradable and non-toxic excipients. Further, we optimized the excipient composition for compatibility and solubility, incorporating higher amounts of levofloxacin in NLC than that described for lipid nanoparticles in the published literature. Solid state analysis indicated that the NLCs had a lipid core with most LV solubilized in it, and the outside was more hydrophilic, containing the remaining LV molecules dispersed in a lamellar-like construction. From the process DoE we found that LV impurities, mainly LNO, could be present in different concentrations in the NLCs depending on the CPPs (sonication time, amplitude and temperature). The LNO degradation product has no antimicrobial activity and could affect the final drug dose, which highlights the need for stability indicating methods when formulating LV.

We prepared an optimized NLC with the adjusted process parameters (58 °C, 20 min sonication time and 50% sonication amplitude) and accelerated studies revealed that LV-loaded NLC was stable according to the preset CQAs for 30 days (40 °C/75% RH) with no significant changes in the particle size, polydispersibility, zeta potential and EE. Total impurities increased 1.7-fold after 30 days at accelerated stability conditions, but it was mainly LV degradation from non-entrapped drug, indicating the drug-protective action of NLC. LV presented a fast release from NLC upon dilution in buffer, but sustained release by the Franz cell method, indicating a preferential use in mucous membranes, such as administration by pulmonary or nasal routes. Independent of the release method, approximately 10-15% of LV remained in the NLCs, which can boost LV internalization and consequently improve intracellular bacterial killing.

5. Acknowledgements

This study was part-financed by the Coordenação de Aperfeiçoamento de Pessoal de Nível Superior - Brasil (CAPES) - Finance Code 001, CAPES-PrInt, Santander – Program of International Mobility number 31/2018 and Sao Paulo Research Foundation (FAPESP) grant numbers 2018/03666-3, 2019/09719-4 and 2020/08059-8. LT and AU acknowledge funding from Science Foundation Ireland, grants 15/CDA/3602 and 12/RC/2275_P2.

References

Abdel Hady, M., Sayed, O.M., Akl, M.A., 2020. Brain uptake and accumulation of new levofloxacin-doxycycline combination through the use of solid lipid nanoparticles: Formulation; Optimization and in-vivo evaluation. Colloids Surfaces B Biointerfaces

193, 111076. https://doi.org/10.1016/j.colsurfb.2020.111076

Ameeduzzafar, Imam, S.S., Abbas Bukhari, S.N., Ahmad, J., Ali, A., 2018. Formulation and optimization of levofloxacin loaded chitosan nanoparticle for ocular delivery: In-vitro characterization, ocular tolerance and antibacterial activity. Int. J. Biol. Macromol. 108, 650–659. https://doi.org/10.1016/j.ijbiomac.2017.11.170

Barbosa, J.P., Neves, A.R., Silva, A.M., Barbosa, M.A., Salette Reis, M., Santos, S.G., 2016. Nanostructured lipid carriers loaded with resveratrol modulate human dendritic cells. Int. J. Nanomedicine 11, 3501–3516. https://doi.org/10.2147/IJN.S108694

Beraldo-de-Araújo, V.L., Beraldo-de-Araújo, A., Costa, J.S.R., Pelegrine, A.C.M., Ribeiro, L.N.M., Paula, E. de, Oliveira-Nascimento, L., 2019. Excipient-excipient interactions in the development of nanocarriers: an innovative statistical approach for formulation decisions. Sci. Rep. 9, 10738. https://doi.org/10.1038/s41598-019-47270-w

Bhalekar, M., Upadhaya, P., Madgulkar, A., 2017. Formulation and characterization of solid lipid nanoparticles for an anti-retroviral drug darunavir. Appl. Nanosci. 7, 47–57. https://doi.org/10.1007/s13204-017-0547-1

Brillault, J., Tewes, F., Couet, W., Olivier, J.C., 2017. In vitro biopharmaceutical evaluation of ciprofloxacin/metal cation complexes for pulmonary administration. Eur. J. Pharm. Sci. 97, 92–98. https://doi.org/10.1016/j.ejps.2016.11.011

Chen, X., Zhang, L., Hu, X., Lin, X., Zhang, Y., Tang, X., 2015. Formulation and preparation of a stable intravenous disulfiram-loaded lipid emulsion. Eur. J. Lipid Sci. Technol. 117, 869–878. https://doi.org/10.1002/ejlt.201400278

Cunha, S., Costa, C.P., Moreira, J.N., Sousa Lobo, J.M., Silva, A.C., 2020. Using the quality by design (QbD) approach to optimize formulations of lipid nanoparticles and nanoemulsions: A review. Nanomedicine Nanotechnology, Biol. Med. 28, 102206. https://doi.org/10.1016/j.nano.2020.102206

Czyrski, A., Anusiak, K., Teżyk, A., 2019. The degradation of levofloxacin in infusions exposed to daylight with an identification of a degradation product with HPLC-MS. Sci. Rep. 9, 3621. https://doi.org/10.1038/s41598-019-40201-9

Das, S., Ng, W.K., Kanaujia, P., Kim, S., Tan, R.B.H., 2011. Formulation design, preparation and physicochemical characterizations of solid lipid nanoparticles containing a hydrophobic drug: Effects of process variables. Colloids Surfaces B Biointerfaces 88, 483–489. https://doi.org/10.1016/j.colsurfb.2011.07.036

Dhiman, N., Awasthi, R., Sharma, B., Kharkwal, H., Kulkarni, G.T., 2021. Lipid Nanoparticles as Carriers for Bioactive Delivery. Front. Chem. 9, 580118. https://doi.org/10.3389/fchem.2021.580118

Fang, J.Y., Fang, C.L., Liu, C.H., Su, Y.H., 2008. Lipid nanoparticles as vehicles for topical psoralen delivery: Solid lipid nanoparticles (SLN) versus nanostructured lipid carriers (NLC). Eur. J. Pharm. Biopharm. 70, 633–640. https://doi.org/10.1016/j.ejpb.2008.05.008

Ferreira, M., Chaves, L.L., Lima, S.A.C., Reis, S., 2015. Optimization of nanostructured lipid carriers loaded with methotrexate: A tool for inflammatory and cancer therapy. Int. J. Pharm. 492, 65–72. https://doi.org/10.1016/j.ijpharm.2015.07.013

Finbloom, J.A., Sousa, F., Stevens, M.M., Desai, T.A., 2020. Engineering the drug carrier biointerface to overcome biological barriers to drug delivery. Adv. Drug Deliv. Rev. 167, 89–108. https://doi.org/10.1016/j.addr.2020.06.007

Garbuzenko, O.B., Kuzmov, A., Taratula, O., Pine, S.R., Minko, T., 2019. Strategy to

enhance lung cancer treatment by five essential elements: Inhalation delivery, nanotechnology, tumor-receptor targeting, chemo- and gene therapy. Theranostics 9, 8362–8376. https://doi.org/10.7150/thno.39816

Gelperina, S., Kisich, K., Iseman, M.D., Heifets, L., 2005. The potential advantages of nanoparticle drug delivery systems in chemotherapy of tuberculosis. Am. J. Respir. Crit. Care Med. 172, 1487–1490. https://doi.org/10.1164/rccm.200504-613PP

Ghasemiyeh, P., Mohammadi-Samani, S., 2018. Solid lipid nanoparticles and nanostructured lipid carriers as novel drug delivery systems: Applications, advantages and disadvantages. Res. Pharm. Sci. 13, 288–303. https://doi.org/10.4103/1735-5362.235156

Gorman, E.M., Samas, B., Munson, E.J., 2012. Understanding the Dehydration of Levofloxacin Hemihydrate. J. Pharm. Sci. 101, 3319–3330. https://doi.org/10.1002/jps.23200

Grillon, A., Schramm, F., Kleinberg, M., Jehl, F., 2016. Comparative activity of ciprofloxacin, levofloxacin and moxifloxacin against Klebsiella pneumoniae, Pseudomonas aeruginosa and Stenotrophomonas maltophilia assessed by minimum inhibitory concentrations and time-kill studies. PLoS One 11, e0156690. https://doi.org/10.1371/journal.pone.0156690

Hamdani, J., Moës, A.J., Amighi, K., 2003. Physical and thermal characterisation of Precirol® and Compritol® as lipophilic glycerides used for the preparation of controlled-release matrix pellets. Int. J. Pharm. 260, 47–57. https://doi.org/10.1016/S0378-5173(03)00229-1

Hejri, A., Khosravi, A., Gharanjig, K., Hejazi, M., 2013. Optimisation of the formulation of β-carotene loaded nanostructured lipid carriers prepared by solvent diffusion method. Food Chem. 141, 117–123. https://doi.org/10.1016/j.foodchem.2013.02.080

Inoue, T., Hisatsugu, Y., Yamamoto, R., Suzuki, M., 2004. Solid-liquid phase behavior of binary fatty acid mixtures: 1. Oleic acid/stearic acid and oleic acid/behenic acid mixtures. Chem. Phys. Lipids 127, 143–152. https://doi.org/10.1016/j.chemphyslip.2003.09.014

Islan, G.A., Tornello, P.C., Abraham, G.A., Duran, N., Castro, G.R., 2016. Smart lipid nanoparticles containing levofloxacin and DNase for lung delivery. Design and characterization. Colloids Surfaces B Biointerfaces 143, 168–176. https://doi.org/10.1016/j.colsurfb.2016.03.040

James H. Young and G. L. Nelson, 1967. Theory of Hysteresis Between Sorption and Desorption Isotherms in Biological Materials. Trans. ASAE 10, 0260–0263. https://doi.org/10.13031/2013.39649

Jannin, V., Pochard, E., Chambin, O., 2006. Influence of poloxamers on the dissolution performance and stability of controlled-release formulations containing Precirol® ATO 5. Int. J. Pharm. 309, 6–15. https://doi.org/10.1016/j.ijpharm.2005.10.042

Kelidari, H.R., Saeedi, M., Akbari, J., Morteza-semnani, K., Valizadeh, H., Maniruzzaman, M., Farmoudeh, A., Nokhodchi, A., 2017. Development and Optimisation of Spironolactone Nanoparticles for Enhanced Dissolution Rates and Stability. AAPS PharmSciTech 18, 1469–1474. https://doi.org/10.1208/s12249-016-0621-0

Khanum, R., Thevanayagam, H., 2017. Lipid peroxidation: Its effects on the formulation and use of pharmaceutical emulsions. Asian J. Pharm. Sci. 12, 401–411. https://doi.org/10.1016/j.ajps.2017.05.003

Kitaoka, H., Wada, C., Moroi, R., Hakusui, H., 1995. Effect of Dehydration on the Formation of Levofloxacin Pseudopolymorphs. Chem. Pharm. Bull. 43, 649–653. https://doi.org/10.1248/cpb.43.649

Koeppe, M.O., Cristofoletti, R., Fernandes, E.F., Storpirtis, S., Junginger, H.E., Kopp, S., Midha, K.K., Shah, V.P., Stavchansky, S., Dressman, J.B., Barends, D.M., 2011. Biowaiver monographs for immediate release solid oral dosage forms: Levofloxacin. J. Pharm. Sci. 100, 1628–1636. https://doi.org/10.1002/jps.22413

Kumar, G., Sharma, S., Shafiq, N., Khuller, G.K., Malhotra, S., 2012. Optimization, in vitro-in vivo evaluation, and short-term tolerability of novel levofloxacin-loaded PLGA nanoparticle formulation. J. Pharm. Sci. 101, 2165–2176. https://doi.org/10.1002/jps.23087

Levofloxacin, 2017. , in: Unites States Pharmacopeia. pp. 4831–4833. https://doi.org/10.1001/jama.1950.02910390046012

Li, J., Qiao, Y., Wu, Z., 2017. Nanosystem trends in drug delivery using quality-by-design concept. J. Control. Release 256, 9–18. https://doi.org/10.1016/j.jconrel.2017.04.019

Liu, H.H., 2010. Safety profile of the fluoroquinolones: Focus on levofloxacin. Drug Saf. 33, 353–369. https://doi.org/10.2165/11536360-000000000-00000

Liu, Y., He, Q., Wu, M., 2015. Levofloxacin-induced crystal nephropathy. Nephrology 20, 437–438. https://doi.org/10.1111/nep.12405

Magenheim, B., Levy, M.Y., Benita, S., 1993. A new in vitro technique for the evaluation of drug release profile from colloidal carriers - ultrafiltration technique at low pressure. Int. J. Pharm. 94, 115–123. https://doi.org/10.1016/0378-5173(93)90015-8

Martins, S., Tho, I., Souto, E., Ferreira, D., Brandl, M., 2012. Multivariate design for the evaluation of lipid and surfactant composition effect for optimisation of lipid nanoparticles. Eur. J. Pharm. Sci. 45, 613–623. https://doi.org/10.1016/j.ejps.2011.12.015

Mesallati, H., Umerska, A., Paluch, K.J., Tajber, L., 2017. Amorphous Polymeric Drug Salts as Ionic Solid Dispersion Forms of Ciprofloxacin. Mol. Pharm. 14, 2209–2223. https://doi.org/10.1021/acs.molpharmaceut.7b00039

Mesallati, H., Umerska, A., Tajber, L., 2019. Fluoroquinolone amorphous polymeric salts and dispersions for veterinary uses. Pharmaceutics 11. https://doi.org/10.3390/pharmaceutics11060268

Müller, R.H., Mäder, K., Gohla, S., 2000. Solid lipid nanoparticles (SLN) for controlled drug delivery - A review of the state of the art. Eur. J. Pharm. Biopharm. 50, 161–177. https://doi.org/10.1016/S0939-6411(00)00087-4

Newman, A.W., Reutzel-Edens, S.M., Zografi, G., 2008. Characterization of the "hygroscopic" properties of active pharmaceutical ingredients. J. Pharm. Sci. 97, 1047–1059. https://doi.org/10.1002/jps.21033

Nguyen, H.A., Grellet, J., Paillard, D., Dubois, V., Quentin, C., Saux, M.-C., 2006. Factors influencing the intracellular activity of fluoroquinolones: a study using levofloxacin in a Staphylococcus aureus THP-1 monocyte model. J. Antimicrob. Chemother. 57, 883–890. https://doi.org/10.1093/jac/dkl079

Nicoletti, M.A., Siqueira, E.L., Bombana, A.C., de Oliveira, G.G., 2009. Shelf-life of a 2.5% sodium hypochlorite solution as determined by arrhenius equation. Braz. Dent. J. 20, 27–31. https://doi.org/10.1590/s0103-64402009000100004

Nisar, J., Iqbal, Mudassir, Iqbal, Munawar, Shah, A., Akhter, M.S., Sirajuddin, Khan, R.A., Uddin, I., Shah, L.A., Khan, M.S., 2020. Decomposition kinetics of levofloxacin: Drug-excipient interaction. Zeitschrift fur Phys. Chemie 234, 117–128. https://doi.org/10.1515/zpch-2018-1273

Nonomura, Y., Nakayama, K., Aoki, Y., Fujimori, A., 2009. Phase behavior of bile acid/lipid/water systems containing model dietary lipids. J. Colloid Interface Sci. 339, 222–229. https://doi.org/10.1016/j.jcis.2009.07.030

Ortiz-Collazos, S., Picciani, P.H.S., Oliveira, O.N., Pimentel, A.S., Edler, K.J., 2019. Influence of levofloxacin and clarithromycin on the structure of DPPC monolayers. Biochim. Biophys. Acta - Biomembr. 1861, 182994. https://doi.org/10.1016/j.bbamem.2019.05.016

Papadimitriou, S., Bikiaris, D., 2009. Novel self-assembled core-shell nanoparticles based on crystalline amorphous moieties of aliphatic copolyesters for efficient controlled drug release. J. Control. Release 138, 177–184. https://doi.org/10.1016/j.jconrel.2009.05.013

Rasmussen, M.K., Pedersen, J.N., Marie, R., 2020. Size and surface charge characterization of nanoparticles with a salt gradient. Nat. Commun. 11, 2337. https://doi.org/10.1038/s41467-020-15889-3

Rezigue, M., 2020. Lipid and Polymeric Nanoparticles: Drug Delivery Applications. pp. 167–230. https://doi.org/10.1007/978-3-030-36260-7_7

Schwarz, C., Mehnert, W., Lucks, J.S., Müller, R.H., 1994. Solid lipid nanoparticles (SLN) for controlled drug delivery. I. Production, characterization and sterilization. J. Control. Release 30, 83–96. https://doi.org/10.1016/0168-3659(94)90047-7

Seedher, N., Agarwal, P., 2010. Effect of metal ions on some pharmacologically relevant interactions involving fl uoroquinolone antibiotics. Drug Metabol. Drug Interact. 25, 17–24. https://doi.org/10.1515/DMDI.2010.003

Shah, S.R., Prajapati, H.R., Sheth, D.B., Gondaliya, E.M., Vyas, A.J., Soniwala, M.M., Chavda, J.R., 2020. Pharmacokinetics and in vivo distribution of optimized PLGA nanoparticles for pulmonary delivery of levofloxacin. J. Pharm. Pharmacol. 72, 1026–1037. https://doi.org/10.1111/jphp.13275

Skoglund, S., Hedberg, J., Yunda, E., Godymchuk, A., Blomberg, E., Odnevall Wallinder, I., 2017. Difficulties and flaws in performing accurate determinations of zeta potentials of metal nanoparticles in complex solutions - Four case studies. PLoS One 12, e0181735. https://doi.org/10.1371/journal.pone.0181735

Subramaniam, B., Siddik, Z.H., Nagoor, N.H., 2020. Optimization of nanostructured lipid carriers: understanding the types, designs, and parameters in the process of formulations. J. Nanoparticle Res. 22, 141. https://doi.org/10.1007/s11051-020-04848-0

Tamjidi, F., Shahedi, M., Varshosaz, J., Nasirpour, A., 2014. EDTA and α-tocopherol improve the chemical stability of astaxanthin loaded into nanostructured lipid carriers. Eur. J. Lipid Sci. Technol. 116, 968–977. https://doi.org/10.1002/ejlt.201300509

Thapa, R.K., Diep, D.B., Tønnesen, H.H., 2021. Nanomedicine-based antimicrobial peptide delivery for bacterial infections: recent advances and future prospects. J. Pharm. Investig. 51, 377–398. https://doi.org/10.1007/s40005-021-00525-z

Torge, A., Wagner, S., Chaves, P.S., Oliveira, E.G., Guterres, S.S., Pohlmann, A.R., Titz, A., Schneider, M., Beck, R.C.R., 2017. Ciprofloxacin-loaded lipid-core nanocapsules as mucus penetrating drug delivery system intended for the treatment of bacterial infections in cystic fibrosis. Int. J. Pharm. 527, 92–102.

https://doi.org/10.1016/j.ijpharm.2017.05.013

Umerska, A., Bialek, K., Zotova, J., Skotnicki, M., Tajber, L., 2020a. Anticrystal engineering of ketoprofen and ester local anesthetics: Ionic liquids or deep eutectic mixtures? Pharmaceutics 12, 368. https://doi.org/10.3390/pharmaceutics12040368

Umerska, A., Cassisa, V., Matougui, N., Joly-Guillou, M.L., Eveillard, M., Saulnier, P., 2016. Antibacterial action of lipid nanocapsules containing fatty acids or monoglycerides as co-surfactants. Eur. J. Pharm. Biopharm. 108, 100–110. https://doi.org/10.1016/j.ejpb.2016.09.001

Umerska, A., Mugheirbi, N.A., Kasprzak, A., Saulnier, P., Tajber, L., 2020b. Carbohydrate-based Trojan microparticles as carriers for pulmonary delivery of lipid nanocapsules using dry powder inhalation. Powder Technol. 364, 507–521. https://doi.org/10.1016/j.powtec.2020.02.028

Wang, D.Y., van der Mei, H.C., Ren, Y., Busscher, H.J., Shi, L., 2020. Lipid-Based Antimicrobial Delivery-Systems for the Treatment of Bacterial Infections. Front. Chem. 7, 872. https://doi.org/10.3389/fchem.2019.00872

Wartewig, S., Neubert, R., Rettig, W., Hesse, K., 1998. Structure of stratum corneum lipids characterized by FT-Raman spectroscopy and DSC. IV. Mixtures of ceramides and oleic acid. Chem. Phys. Lipids 91, 145–152. https://doi.org/10.1016/S0009-3084(97)00105-9

Wei, N., Jia, L., Shang, Z., Gong, J., Gong, J., Wu, S., Wang, J., Tang, W., 2019. Polymorphism of levofloxacin: Structure, properties and phase transformation. CrystEngComm 21, 6196–6207. https://doi.org/10.1039/c9ce00847k

Wooster, T.J., Golding, M., Sanguansri, P., 2008. Impact of oil type on nanoemulsion formation and ostwald ripening stability. Langmuir 24, 12758–12765. https://doi.org/10.1021/la801685v

Zhang, C., Zhao, W., Bian, C., Hou, X., Deng, B., McComb, D.W., Chen, X., Dong, Y., 2019. Antibiotic-Derived Lipid Nanoparticles to Treat Intracellular Staphylococcus aureus. ACS Appl. Bio Mater. 2, 1270–1277. https://doi.org/10.1021/acsabm.8b00821

Declaration of interests

☒ The authors declare that they have no known competing financial interests or personal relationships that could have appeared to influence the work reported in this paper.

☐ The authors declare the following financial interests/personal relationships which may be considered as potential competing interests:

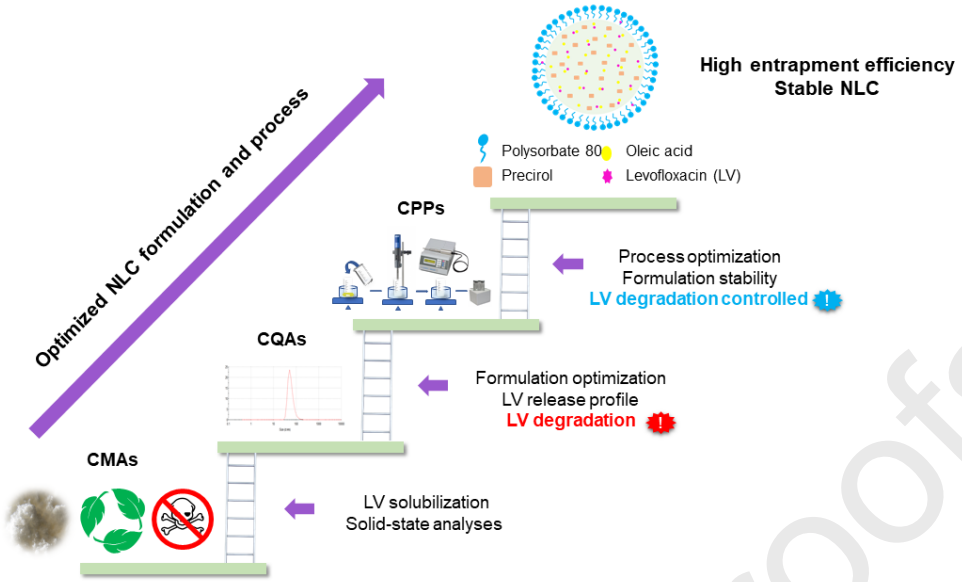

CMAs: Critical Material Attributes; **CQAs**: Critical Quality Attributes; **CPPs**: Critical Process Parameters